N 77-18095

ATMOSPHERIC TURBULENCE POWER SPECTRAL MEASUREMENTS TO LONG
WAVELENGTHS FOR SEVERAL METEOROLOGICAL CONDITIONS

Richard H. Rhyne and Harold N. Murrow
NASA Langley Research Center

Kenneth Sidwell
The George Washington University
Joint Institute for Advancement of Flight Sciences

SUMMARY

Use of power spectral design techniques for supersonic transports requires accurate definition of atmospheric turbulence in the long wavelength region below the "knee" of the power spectral density function curve. Examples are given of data obtained from a current turbulence flight sampling program. These samples are categorized as (1) convective, (2) wind shear, (3) rotor, and (4) mountain-wave turbulence. Time histories, altitudes, root-mean-square values, statistical degrees of freedom, power spectra, and integral scale values are shown and discussed.

15

INTRODUCTION

"Gustiness" or the effect of atmospheric turbulence has always been of concern for aircraft operations. In early years individual or discrete gusts of differing shape were used to verify designs. It was always recognized that turbulence is a statistical phenomenon, however, in that single gusts are seldom if ever encountered. About 25 years ago the use of random process theory, or more commonly referred to as "power spectral analysis" techniques, began to receive significant attention as a more appropriate design analysis method. As a result of these developments, experimental turbulence sampling programs were conducted in order to provide a statistical description of the atmosphere in power spectral form. These measurements verified, in general, that the slope of the von Karman equation (given in fig. 1) of $-5/3$ is appropriate. Limitations in both instrumentation and data reduction procedures prevented the acquisition of data at wavelengths long enough to identify appropriate values of L in the von Karman equation (or to verify the validity of the equation). If L (generally referred to as the integral scale value and physically sometimes thought of as the average eddy size (ref. 1)) and σ (the root-mean-square value) are known, then the power spectrum is completely described. Regardless of the intensity or power level, each L value corresponds to a specific knee or break frequency in the power spectrum curve. Meteorological researchers therefore need appropriate L values to fill gaps in the description of the atmosphere. An example of the significance of the L value for aircraft designers is shown by the vertical lines in figure 1. (Note that log scales are used in fig. 1.) The primary object of

PRECEDING PAGE BLANK NOT FILMED

response to turbulence is in the rigid body, short period, and Dutch roll modes. For subsonic aircraft such as the 707, B-52, and 747 airplanes which cruise at M ≈ 0.8 and at altitudes of 11 to 12 km (35 000 to 40 000 ft), the primary response to turbulence is to the right of the knee of the spectral curves for all values of L in the range believed to be appropriate for consideration. However, for supersonic cruise aircraft such as are being studied presently in this country, that is, cruise M ≈ 2.7 at approximately 18 km (60 000 ft), the predicted response is more significantly affected by the L value as can be seen in the figure. Fatigue and ride quality are also important aspects of the aircraft response to atmospheric turbulence. It was decided, therefore, that significant effort was warranted to remove this gap in the knowledge of atmospheric turbulence properties and establish a program with a primary aim of determining appropriate values of L for different meteorological conditions. As a result, special attention must be given to instrumentation and data processing in the low-frequency or long-wavelength region.

SYMBOLS

Values are given in both SI and U.S. Customary Units. The measurements and calculations were made in U.S. Customary Units.

g acceleration due to gravity, m/sec^2 (ft/sec^2)

h altitude, km (ft)

L integral scale value, meters (ft)

M Mach number

u longitudinal component of turbulence, m/sec (ft/sec)

v lateral component of turbulence, m/sec (ft/sec)

w vertical component of turbulence, m/sec (ft/sec)

λ wavelength, meters (ft)

σ root-mean-square value (also standard deviation), m/sec (ft/sec)

$\sigma_u, \sigma_v, \sigma_w$ standard deviations of u, v, and w

Φ power spectral density, $\dfrac{(m/sec)^2}{cycles/meter}$ $\left(\dfrac{(ft/sec)^2}{cy/cles/ft}\right)$

PROGRAM IMPLEMENTATION

The NASA MAT (Measurement of Atmospheric Turbulence) program was established in response to the preceding requirements. All three components of turbulence (vertical, lateral, and longitudinal) were to be measured. It was decided that two sampling aircraft would be required to cover the entire altitude range of

272

interest – one airplane covering the range of altitudes from sea level to 15 km (50 000 ft) and a special high-altitude airplane for altitudes above 15 km. The sensors selected required sampling to be done at subsonic speeds. A B-57B Canberra was selected for the sampling at altitudes up to 15 km and it was decided that a B-57F would be the preferred aircraft for use at altitudes above 15 km. Basically, the required measurements for each of the three turbulence components involve a primary measurement on a boom forward of the aircraft (see fig. 2) (angle fluctuations for the vertical and lateral and airspeed variations for the longitudinal components of the turbulence) which must then be corrected for aircraft motion. Motion corrections are provided by data from an onboard inertial platform and from rate gyros. These corrections are especially important, the present emphasis being on accurate data at long wavelengths. The equations are given in reference 2. To obtain power estimates at the extremely low frequencies required (that is, long wavelengths), narrow spectral "windows" (bandwidths) on the order of 0.02 Hz must be used in the data processing procedure. Such narrow spectral windows introduce wild statistical fluctuations in the power estimates unless relatively long data samples can be obtained. The statistical reliability believed to be necessary requires on the order of 24 to 30 statistical degrees of freedom for the spectral values and translates to data samples of at least 19-minute duration. The instrumented B-57B sampling airplane is shown in figure 3. Details concerning the power spectral algorithms employed, and the justification for not prewhitening the time histories for long wavelength analysis are given in reference 3. Instrumentation details and measurement accuracies are given in reference 4. An assessment of the overall instrumentation performance be ... of inflight maneuvers, together with an assessment of possible low-frequency trend type errors based upon postflight performance of the inertial platform system, is given in reference 5.

Sampling flights with the B-57B were ... on the March 1975 to September 1975 time period. A total of 46 flights ... made, 30 in Eastern United States within range of the airplane based at Langley Air Force Base, Virginia and 16 in Western United States within range ... base at Edwards Air Force Base, California. A full time pr ... meteorologist provided functions of coordinating and planning flights, observing from the rear seat during the flight ..., and conducting postflight ... to ... pertinent meteorological parameters and to define the meteorological conditions where turbulence was encountered.

A summary of data obtained is given ... with the number of data runs to be processed associated with each ... logical conditions. Data processing is currently in process ... four samples (identified by asterisks in table 1) have been selected for detailed discussion in this paper.

DATA PRESENTATION AND DISCUSSION

The four cases selected for detailed discussion herein are categorized according to meteorological condition. (The mountain wave case appears to also involve some wind shear and thus probably should not be considered to be a pure classical case of mountain-wave turbulence.) Pertinent information for the four cases is summarized in table 1. ... run lengths are given for the four ... and, associated with the run lengths, the statistical degrees of freedom (ref. 6)

appropriate for the resulting power spectra are also given. It was a goal in this program to achieve at least 24 statistical degrees of freedom with a resolution bandwidth of 0.02 Hz. Note that for the rotor case, the goal was not quite achieved; thus, somewhat larger random-type fluctuations can be expected in these power spectral estimates. Root-mean-square (σ) values for the three components of turbulence (longitudinal (u), lateral (v), and vertical (w)) are also given in table II. Note that for the convective and perhaps the rotor case, the σ values are similar for the three components. However, for the wind-shear and mountain-wave cases the vertical component has a much smaller σ value than that of the lateral component by factors of 3 to 4 which indicates a lack of isotropy. This aspect will be discussed later in the paper. Data to be presented and discussed for the four cases will include time histories, power spectra, and exceedance curves.

Time histories for the convective case at an altitude of 0.3 km (1000 ft) above gently rolling terrain are given in figure 4. Because of the length of this run (19.1 minutes), the first part of the time histories is shown in figure 4(a) and the final portion in figure 4(b). As shown in table II, the σ values are similar for the three components and are about 1.2 m/s (4 fps).

The power spectra resulting from these time histories are shown in figure 5. The curves are comparable to those of figure 1 except that the results have not been normalized; that is, the area under the curves is equal to the variance or σ^2. The abscissa values were obtained by converting frequency to inverse wavelength by use of the average true airspeed for each run. Symbols are shown for the five lowest frequency power estimates. Except for the first point, which will be discussed subsequently, the estimates are at equal increments of approximately 0.01 Hz (10 Hz/1024). On a log plot the points therefore appear closer together at higher values of $1/\lambda$. The first point is obtained from the data-reduction algorithm at zero frequency but, for convenience, is located at one-fourth the interval between zero and the next regularly obtained point at 0.01 Hz, or at 0.0025 Hz. (The value could not, of course, be shown at zero frequency on a logarithmic plot.) These zero-frequency power estimates are believed to be valid for the results presented in this paper. (See ref. 5.) Past practice has been to discard this value because of the effect of trend errors in the time histories, and because the prewhitening procedure used at that time for wide-band spectral analysis caused the value to go to infinity. Superimposed on the data are shown theoretical von Karman type curves with selected L values. Note that the slopes of the curves match at the higher frequencies. It is shown that the vertical component can be described very accurately with an L value of 300 m (1000 ft). The lateral component, however, has relatively higher power content at low frequencies and the appropriate L value is apparently in the range of 600 m (2000 ft). The longitudinal component fits well with an L value of 1200 m (4000 ft). This difference between components, of course, means that the turbulence is not isotropic in the long wavelength region. In the wavelength region where previous measurements have been made, however, isotropy would seem to prevail.

The time histories for the high-altitude wind-shear case are presented in figure 6. It should be noted that the vertical-scale sensitivities have been decreased by a factor of 2 as compared with the preceding case and that the

severity is much greater. The intensity of the turbulence for all three components is gradually increasing with time. Such nonhomogeneous (or nonstationary) behavior has generally been believed to be responsible for considerable rounding or smoothing of the spectral knee. The recent work of reference 7, however, indicates that unless the change in intensity is considerably more abrupt than shown here, little effect should be observable in the spectra. It is obvious that significant low-frequency power is present in the horizontal components; this is assumed to be directly attributable to the changing horizontal wind field. The low-frequency content can be thought of as a modulation of the mean value with a typical high-frequency amplitude-modulated random process superimposed. A model of turbulence which includes mean modulation has been suggested by Reeves (ref. 8). No pronounced low-frequency power is noted in the vertical component. These observations are substantiated in the corresponding power spectra shown in figure 7. Note that while an L value of 300 m (1000 ft) appears to be appropriate for the vertical component, L values of greater than 1800 m (6000 ft) would apply for the horizontal components directly reflecting the large power content at low frequencies.

The next case to be presented was an encounter on the lee side of the Sierra Mountains in California at an altitude approximately level with the higher ridges. The turbulence was categorized as rotor-type turbulence. The onboard observer reported direct correlation of turbulence severity with the upwind terrain. Peak center-of-gravity acceleration increments of 1g were equaled or exceeded 80 times in this traverse of the rotor region, with maximum incremental accelerations of +2.2g and -1.8g. Time histories of the three components of turbulence are given in figure 8. Note the segments between $4\frac{1}{2}$ and $7\frac{1}{2}$ minutes for the longitudinal component where high-frequency oscillations are absent. This condition is caused by the sensitive airspeed measurement system being off-scale some of the time in the negative direction; as a result, the high-frequency fluctuations were partially lost. It can be seen that relatively low-frequency wavelike oscillations are present on all three time histories, the lateral component exhibiting the most prevalent and highest amplitude oscillations. The σ values given in table II further substantiate this observation. The spectra for this case are given in figure 9. All three spectra continue upward with large low-frequency power; thus, if the von Karman expression is applicable in this region, L must be greater than 1800 m (6000 ft). It should be noted that the high-frequency part of the longitudinal spectrum, as well as σ_u, could be somewhat contaminated by the loss of the high-frequency fluctuations as a result of the partial off-scale condition previously mentioned. The flattening-out of the high-frequency end of the spectrum is not associated with this problem but is a result of the use of the high-altitude restrictor provided for the pitot-static test head. The use of two different restrictors for flight operations above and below 9.1 km (30 000 ft) to provide the proper damping for the sensitive airspeed measurement is discussed in reference 4. In this particular case the high-altitude restrictor was installed, since the original mission for this flight was to seek high-altitude mountain-wave turbulence.

The final case considered herein is categorized as lee wave-generated turbulence which propagated upward and was encountered at an altitude of about 14.3 km (47 000 ft). The time histories are given in figure 10. Notice that the vertical component contains at least three waves and possibly four. Patches of turbulence

occur on the rising part of the last two waves; or at approximately $7\frac{1}{2}$ and 10 minutes from the start of the run. Apparently, the last two waves have not broken down into continuous turbulence as yet, or the displacement of the airplane has carried it out of the turbulent region of the wave. Inspection of the lateral and longitudinal components, where a very long wave can be seen, together with supplementary meteorological information, indicates that wind-shear effects were also present. Thus, this is not a classic case of pure mountain-wave turbulence. These time histories are of considerable interest; whether they should be used to obtain power spectra might be debatable since the turbulence is not very continuous. Power spectra were obtained, however, for the whole 12.6-minute run and are shown in figure 11. A large amount of low-frequency power is present in all three components. This case is in contrast to the wind-shear-alone case where the vertical component contained relatively little low-frequency power.

Figure 12 presents the measured exceedances of the vertical velocity component of turbulence for the four cases considered herein. The exceedances are (for each selected level) the average of the crossings of the positive and negative levels about the zero mean value for the data run. Only positive slope crossings are counted. In figure 12, the crossings per unit distance (in both km and mi) are shown on a logarithmic scale with the level of the vertical velocity component on a linear scale. The exceedances reflect the relative turbulence intensity levels of the four cases. The high intensity rotor and high-altitude wind-shear cases show significantly more crossings than the convective and mountain-wave cases; for example, at a level of 5 meters per second the difference is about two orders of magnitude.

The four exceedance curves of figure 12 show a combination of the exponential and Gaussian functional forms which are used for the analysis of atmospheric turbulence data. The exponential form of the exceedance expression has generally been found applicable for extended data samples or composites of many samples. It is the basis for development of structural design criteria for aircraft response to atmospheric turbulence for both the discrete gust approach and the random process or power spectral method. The exponential form would appear as a straight line on the semi-log plot of figure 12. From inspection of the figure, it appears that the high-altitude wind-shear case is the most nearly exponential (linear) and the rotor case would appear to be the most nearly Gaussian.

CONCLUDING REMARKS

Data have been collected for a number of turbulence encounters at altitudes between 0.3 and 15 km (1000 and 50 000 ft). The associated meteorological conditions have been identified. Four encounters were considered herein. For these cases the following observations are made:

1. The von Karman turbulence model seems to be appropriate for the vertical component in the low-altitude convective and high-altitude wind-shear cases, with an integral scale value of 300 m (1000 ft).

276

2. The lateral and longitudinal components appear to also fit the model fairly well for the low-altitude convective case when integral scale values of 600 m (2000 ft) and 1200 m (4000 ft), respectively, are used.

3. For the horizontal components in the high-altitude wind-shear case, and all three components in the rotor case, very large power obtained at the long wavelengths makes it doubtful whether the von Karman expression is applicable in this region. If it is, integral scales values greater than 1800 m (6000 ft) are required.

4. The time histories from the mountain-wave case appeared to include some effects of wind shear. All the "waves" had not broken down into continuous turbulence and were thus probably not especially appropriate for spectral representation. Very large power however was present at long wavelengths.

5. All cases exhibited the -5/3 slope of the von Karman expression in the shorter wavelength region.

6. The turbulence intensity was very severe for the rotor case and approached that of a small thunderstorm.

Data processing and further analysis are continuing. At the present time it is not known whether similar meteorological conditions will result in similar power spectra. The instrumentation system is scheduled to be installed in a B-57F aircraft later this year in order to acquire turbulence samples above 15 km (50 000 ft).

REFERENCES

1. Houbolt, John C.; Steiner, Roy; and Pratt, Kermit G.: Dynamic Response of Airplanes to Atmospheric Turbulence Including Flight Data on Input and Response. NASA TR R-199, 1964.

2. Murrow, Harold N.; and Rhyne, Richard H.: The MAT Project - Atmospheric Turbulence Measurements With Emphasis on Long Wavelengths. Proceedings of the Sixth Conference on Aerospace and Aeronautical Meteorology of the American Meteorological Society, Nov. 1974, pp. 313-316.

3. Keisler, Samuel R.; and Rhyne, Richard H.: An Assessment of Prewhitening in Estimating Power Spectra of Atmospheric Turbulence at Long Wavelengths. NASA TN D-8288, 1976.

4. Meissner, Charles W., Jr.: A Flight Instrumentation System for Atmospheric Turbulence Data. NASA TN D-8314, 1976.

5. Rhyne, Richard H.: Flight Assessment of Atmospheric Turbulence Measurement System With Emphasis on Long Wavelengths. NASA TN D-8315, 1976.

6. Otnes, Robert K.; and Enochson, Loren: Digital Time Series Analysis. John Wiley & Sons, Inc., c.1972.

7. Mark, William D.; and Fischer, Raymond W.: Investigation of the Effects of Nonhomogeneous Behavior on the Spectra of Atmospheric Turbulence. NASA CR-2745, 1976.

8. Reeves, Paul M.; Joppa, Robert G.; and Ganzer, Victor M.: A Non-Gaussian Model of Continuous Atmospheric Turbulence for Use in Aircraft Design. NASA CR-2639, 1976.

TABLE I.- SAMPLING SUMMARY OF B-57B FLIGHTS

[46 FLIGHTS WERE MADE BETWEEN MARCH 1974 AND SEPT. 1975]

(30 EASTERN U.S. AND 16 WESTERN U.S.)

TURBULENCE CATEGORY	NUMBER OF DATA RUNS	
TERRAIN RELATED, ROTOR*	14	(6 FLIGHTS)
THERMAL , CONVECTIVE*	8	(2 FLIGHTS)
NEAR THUNDERSTORMS	12	(2 FLIGHTS)
JET STREAM AND HIGH-ALTITUDE WIND SHEAR*	27	(6 FLIGHTS)
MOUNTAIN WAVES*	8	(4 FLIGHTS)
ISOLATED SITUATIONS	7	(2 FLIGHTS)

* CASES SELECTED FOR REVIEW IN THIS PAPER

TABLE II.- PERTINENT DATA FOR FOUR SELECTED CASES

METEOROLOGICAL CONDITION	ALTITUDE , km (ft)	RUN LENGTH		STATISTICAL d.f. FOR POWER SPECTRA	σ_w , m/sec (ft/sec)	σ_v , m/sec (ft/sec)	σ_u , m/sec (ft/sec)
		min	km (miles)				
CONVECTIVE	0.3 (1000)	19.1	148 (91.7)	45	1.15 (3.78)	1.18 (3.86)	1.35 (4.41)
WIND SHEAR	13.0 (42600)	12.2	137 (85.1)	29	2.45 (8.05)	7.33 (24.03)	4.48 (14.70)
ROTOR	3.9 (12800)	8.1	88.5 (55.0)	19	3.82 (12.52)	5.51 (18.09)	3.57 (11.73)
MOUNTAIN WAVE	14.3 (46800)	12.6	149 (92.4)	29	1.34 (4.41)	5.39 (17.69)	4.30 (14.11)

d.f. = f (BANDWIDTH, LENGTH)
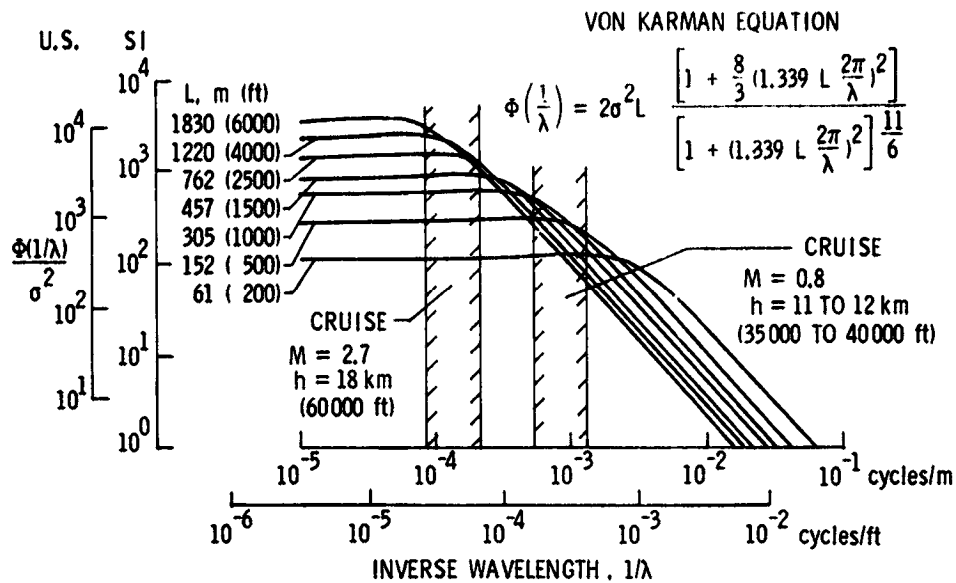
Figure 1.- Wavelength regions of primary aircraft response
shown on von Karman theoretical spectra.
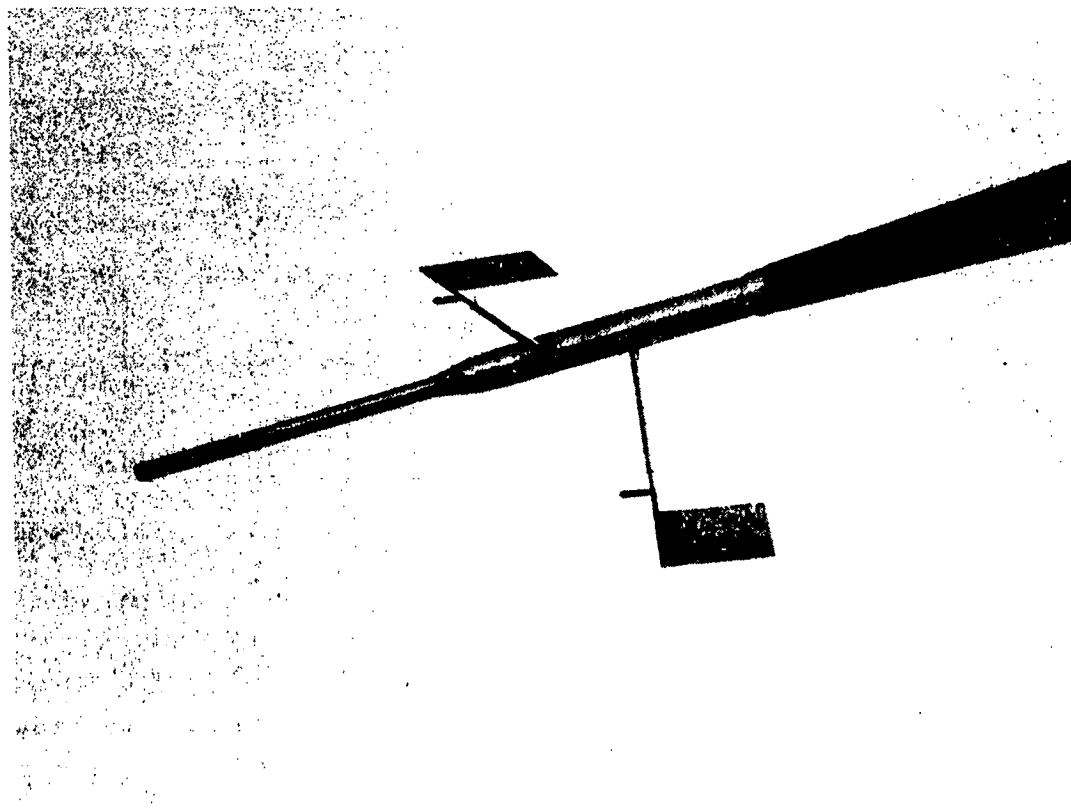
Figure 2.- Head for providing three basic measurements.
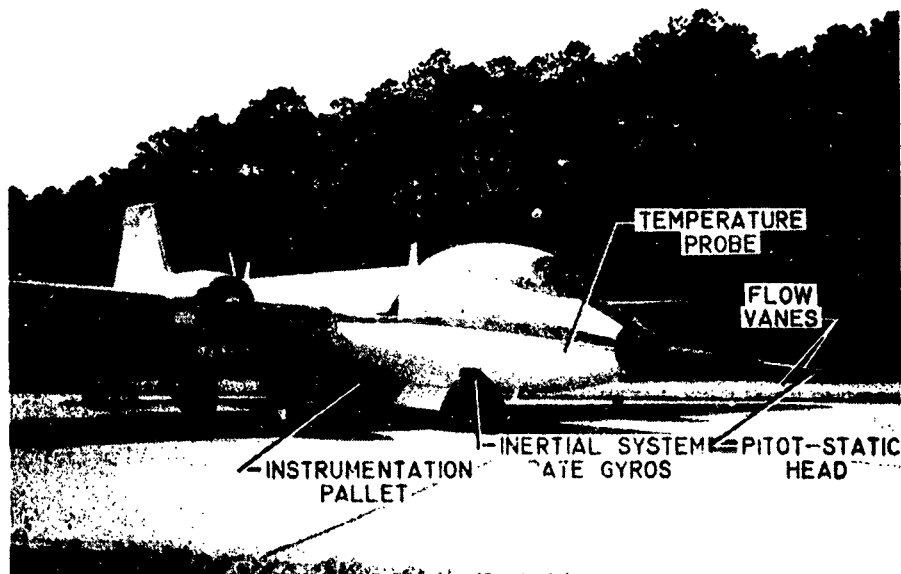
Figure 3.- Instrumented airplane.
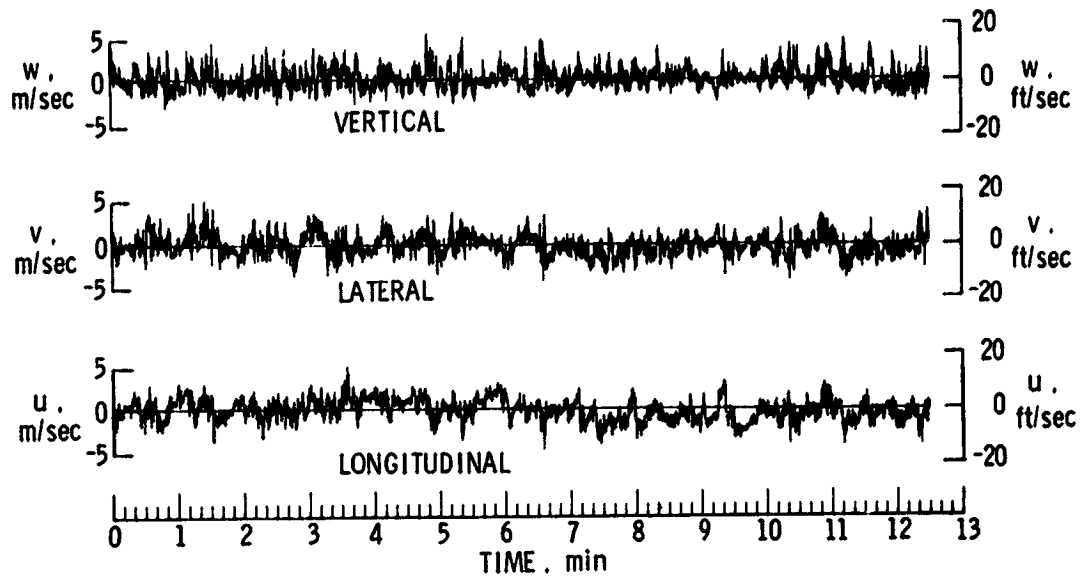
(a) Time interval, 0 to 12.5 minutes.
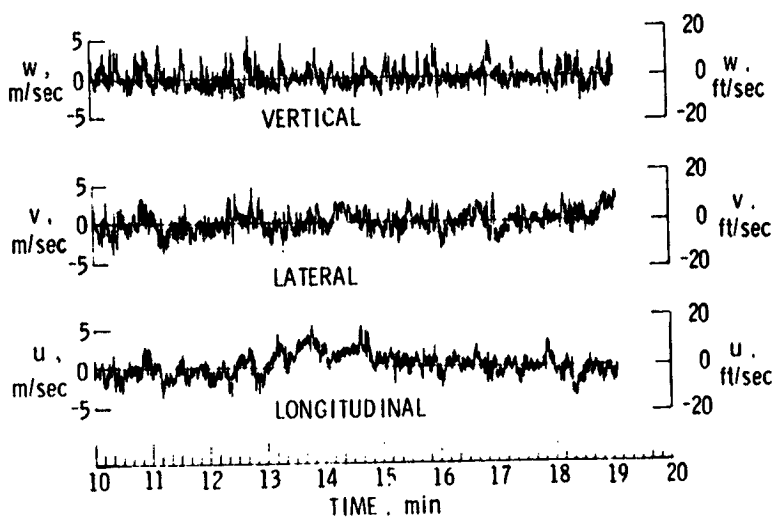
(b) Time interval, 10 to 19 minutes.

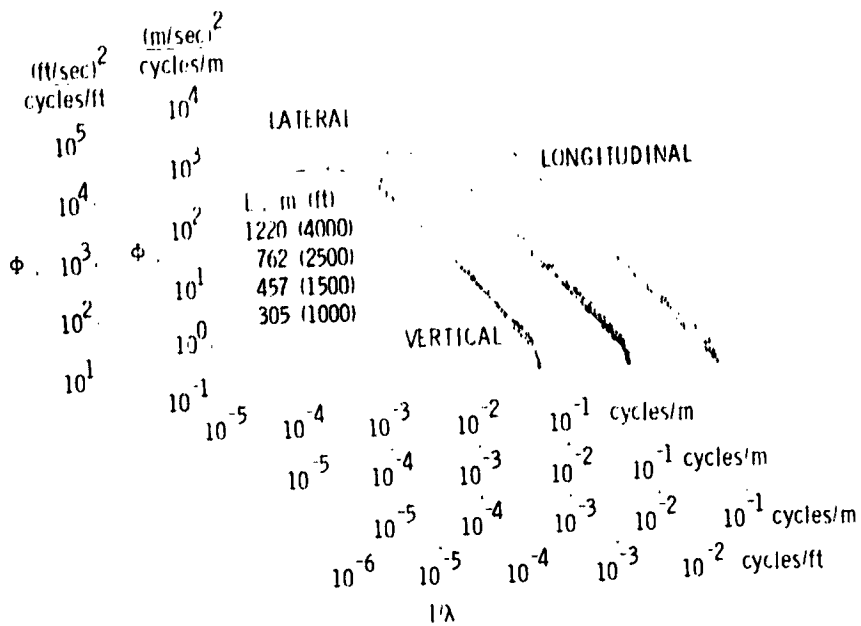Figure 4.- Turbulence component time histories. Convective case.

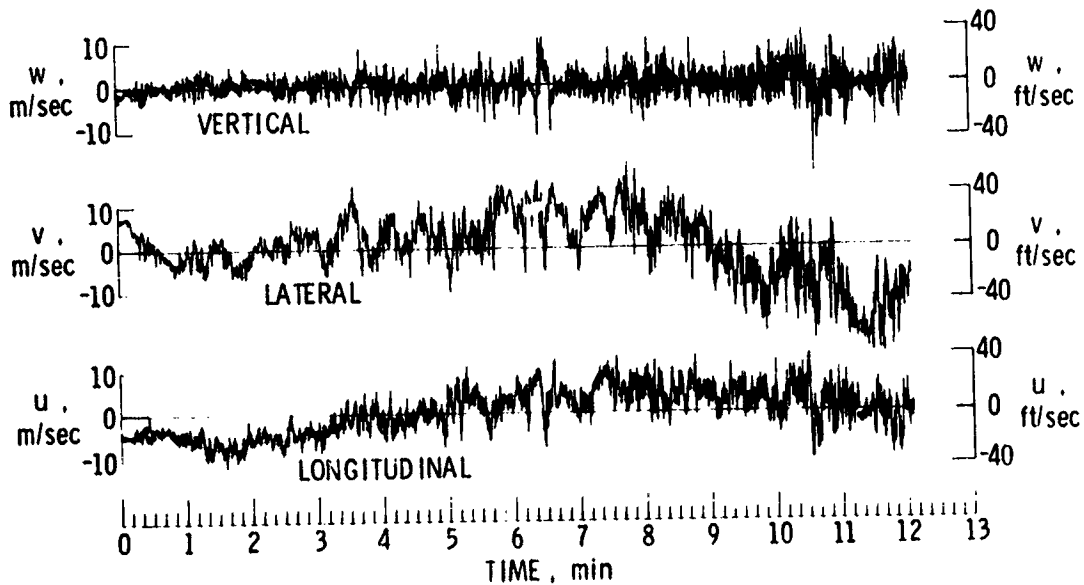Figure 5.- Power spectra of turbulence components.
Convective case.

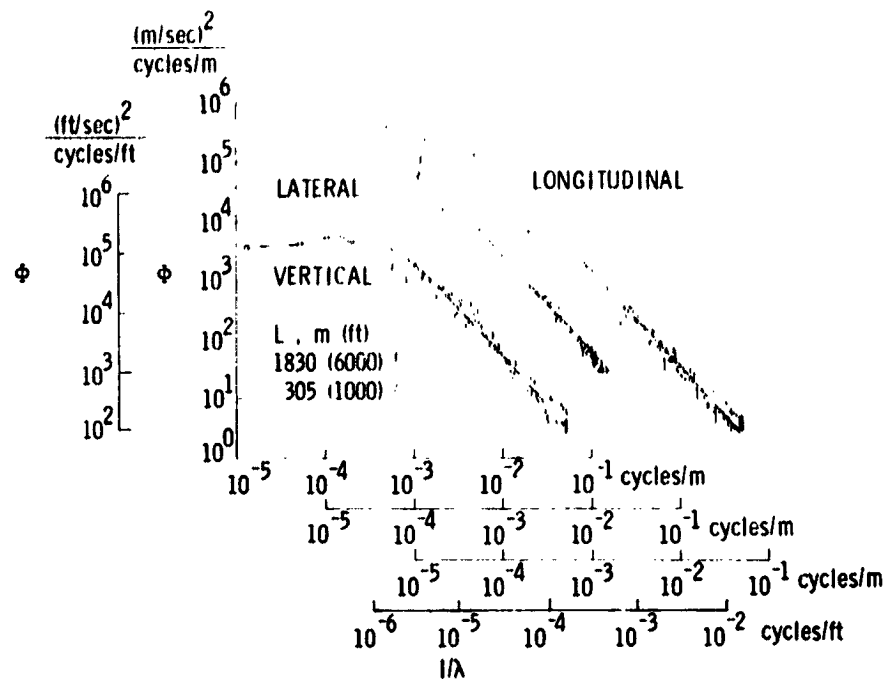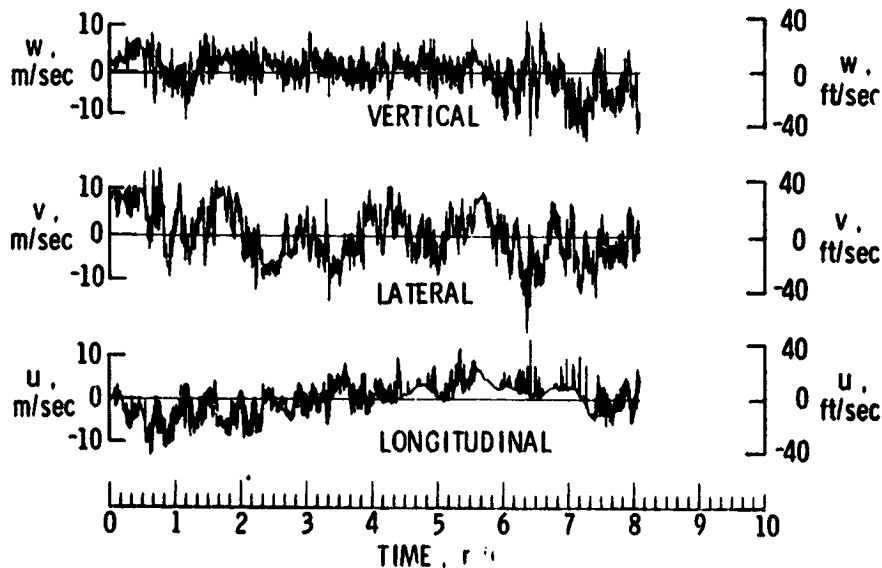Figure 6.- Turbulence component time histories.
High-altitude wind-shear case.

283

Figure 7.- I wer spectra of turbulence components.
High-altitude wind-shear case.
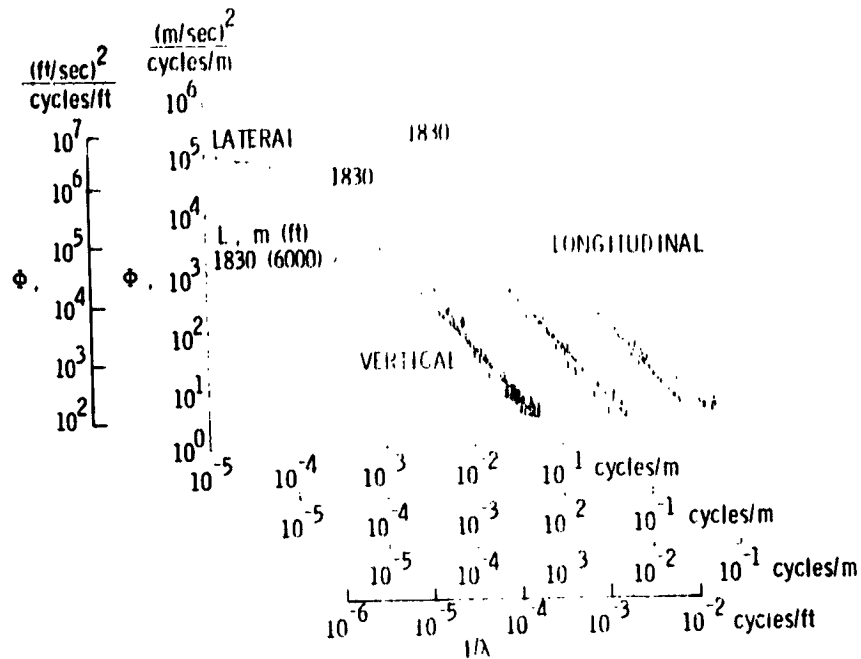

Figure 8.- Turbulence component time histories. Rotor case.

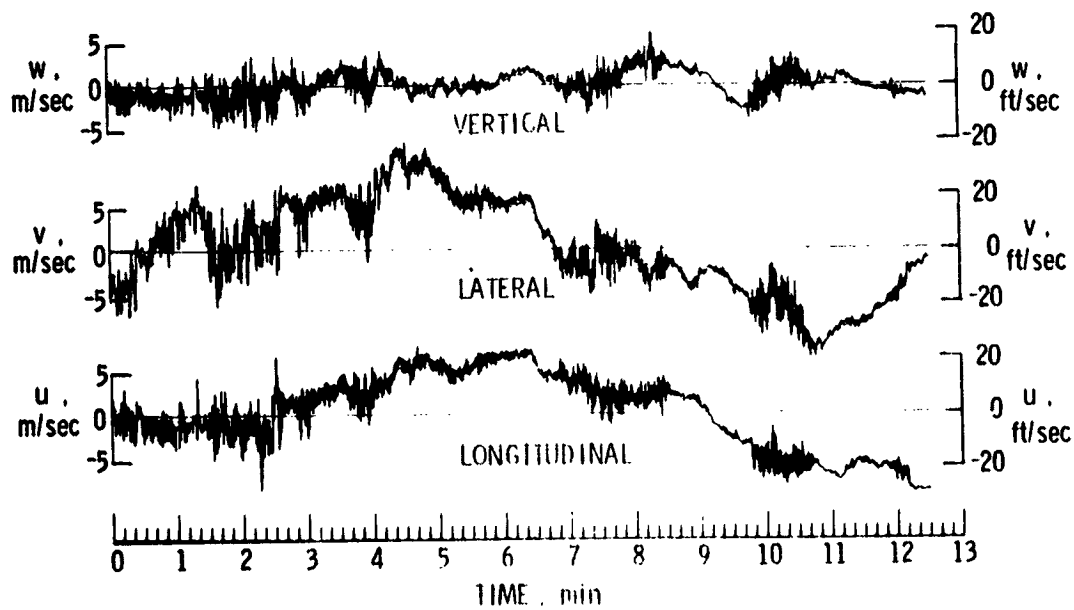Figure 9.- Power spectra of turbulence components. Rotor case.

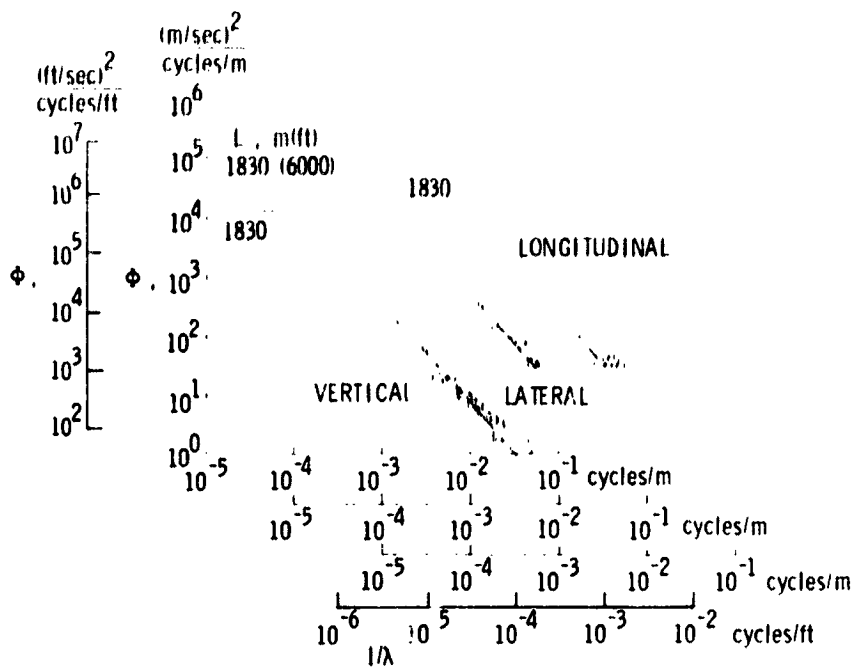Figure 10.- Turbulence component time histories. Mountain-wave case.

Figure 11.- Power spectra of turbulence components.
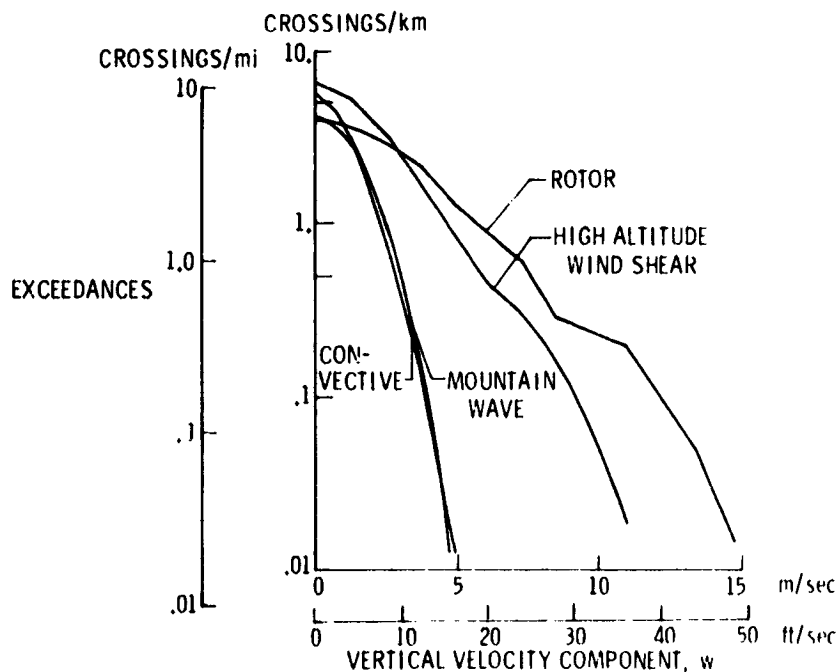Mountain-wave case.

Figure 12.- Measured exceedance frequency of vertical component
of gust velocity for four meteorological cases.